(4) A. Finazzi-Agro, G. Rotilio, L. Aviglionano, P. Guerrieri, V. Boffi, and B. Mondovi, *Biochemistry*, 9, 2009 (1970).
(5) S. Katoh and A. Takamiya, *J. Biochem. (Tokyo)*, 55, 378 (1964).
(6) D. R. McMillin, R. A. Holwerda, and H. B. Gray, *Proc. Natl. Acad. Sci. U.S.A.*, 71, 1339 (1974).
(7) D. R. McMillin, R. C. Rosenberg, and H. B. Gray, *Proc. Natl. Acad. Sci. U.S.A.*, 71, 4760 (1974).
(8) V. Miskowski, S.-P. Tang, T. G. Spiro, E. Shapiro, and T. H. Moss, *Biochemistry*, 14, 1244 (1975).
(9) O. Siiman, N. M. Young, and P. R. Carey, *J. Am. Chem. Soc.*, 96, 5583 (1974).
(10) G. S. Patterson and R. H. Holm, *Bioinorg. Chem.*, 4, 257 (1975).
(11) Y. Sugiura, Y. Hirayama, H. Tanaka, and K. Ishizu, *J. Am. Chem. Soc.*, 97, 5577 (1975); Y. Sugiura, Y. Hirayama, H. Tanaka, and H. Sakurai, *J. Inorg. Nucl. Chem.*, 37, 2367 (1975).
(12) I. Mita, N. Toshioka, and S. Yamato, Japanese Patent 11616 (1964).
(13) D. M. G. Armstrong, *Chem. Ind. (London)*, 1405 (1955).
(14) S. P. Datta and B. R. Rabin, *Trans. Faraday Soc.*, 52, 1123 (1956).
(15) O. Yamauchi, Y. Hirano, Y. Nakao, and A. Nakahara, *Can. J. Chem.*, 47, 3441 (1969).
(16) G. F. Bryce and F. R. N. Gurd, *J. Biol. Chem.*, 241, 122 (1966).
(17) R. G. Pearson, *J. Am. Chem. Soc.*, 85, 3533 (1963).

Molecular Orbital Studies on the Optical Activity of Chiral Four-Coordinate Copper(II) Systems

CHIN-YAH YEH and F. S. RICHARDSON*

The chiroptical properties associated with the d–d and low-lying charge-transfer transitions in several types of dissymmetric four-coordinate Cu^{2+} systems are calculated on a semiempirical molecular orbital model. Of particular interest are systems in which the metal ion–donor group cluster are inherently dissymmetric and metal–ligand π interactions are expected to be significant. Spectra–structure relationships based on correlations of d–d and charge-transfer rotatory strengths with various stereochemical features of chiral Cu^{2+} complexes are developed and discussed. The results demonstrate the sensitivity of both the signs and magnitudes of the chiroptical properties to donor atom sets, configurational distortions of chelate ring systems, chelate ring conformation, and chelate ring substitution (vicinal effects). Useful and reliable correlations between structure parameters and the rotatory strengths of individual transitions are not readily apparent in the calculated results. However, strong correlations between various structure variables and the net d–d (and charge-transfer) rotatory strengths were found.

I. Introduction

Chiroptical spectroscopy has been used extensively to probe the structural details of complexes formed by transition metal ions with a variety of ligand types.[1] The optical activity exhibited by the metal ion d–d transitions and the low-lying (near-ultraviolet) charge-transfer transitions in these systems has been of special interest for developing spectra–structure relationships from which both stereochemical and electronic structural information can be obtained. Although most of the spectra–structure relationships developed and applied so far are based on purely empirical or semiempirical correlations, some effort has been expended in developing a purely theoretical basis for these relationships within the framework provided by various quantum mechanical models of molecular optical activity. These theoretical studies, however, have not produced a fully satisfactory model or theory capable of providing widely applicable and reliable spectra–structure correlations.

Chirality in transition metal complexes is generally attributed to one or more of the following structural features: (1) chiral distortions within the metal ion–donor group cluster ("inherent dissymmetry"); (2) chiral distributions of chelate rings about the metal ion ("configurational dissymmetry"); (3) chiral conformations of chelate rings ("conformational dissymmetry"); (4) asymmetric centers within the ligands (including, in some cases, asymmetric donor atoms). Most theoretical analyses and spectra–structure correlations (such as those based on sector or regional rules) have focused on the latter three sources of chirality, although the possible importance of inherent dissymmetry within the metal ion–donor group cluster has been examined in several studies.

Theoretical treatments of optical activity in chiral transition metal complexes have generally developed along three different lines. In one approach an independent-systems representation of the complex is adopted wherein the complex is partitioned into an achiral chromophoric group (which includes the metal ion) and a set of extrachromophoric groups distributed throughout the ligand environment.[2] Interactions between the chromophoric group and extrachromophoric groups are treated by perturbation techniques, and optical activity in the chromophoric transitions is assumed to arise from dissymmetric terms in these interactions. The theoretical bases for the several sector or regional rules which have been proposed and applied in making spectra–structure correlations in chiral transition metal complexes derive from various forms of the independent-systems model. On this model the chromophore–extrachromophore coupling is assumed to arise from purely electrostatic interactions between nonoverlapping charge distributions on the chromophoric and extrachromophoric groups. Dissymmetry in these interactions can originate with (1) chiral distributions of achiral extrachromophoric groups about the chromophoric center, (2) chiral centers within the perturbing extrachromophoric groups, and (3) a combination of both (1) and (2).

The second approach to examining the origins of optical activity in transition metal complexes focuses on chiral distortions of donor atom orbitals. These distortions reflect the chiral nature of the ligand environment beyond the donor atom set and communicate chirality to the chromophoric electrons of the metal ion via direct bonding (or antibonding) interactions. Liehr[3] and Karipides and Piper[4] adopted this approach and employed a LCAO–MO model for representing the dissymmetrically distorted electronic structure of the metal ion–donor atom cluster. Strickland and Richardson[5] performed a series of calculations based essentially on Liehr's and Piper's models. Schäffer[7] adopted a similar approach in his study of optically active transition metal complexes, but instead of an LCAO–MO model for the electronic structure of the chromophore he employed the angular overlap model.[7]

In the independent-systems model, the chromophoric electrons of the metal ion sense the chirality of the complex via "through-space" electrostatic interactions with the ligand

environment. In Liehr's, Piper's, and Schaffer's models chirality in the ligand environment is communicated to the metal ion through orbital distortions at the donor atoms. The third approach to studying the chiroptical properties of metal complexes involves direct molecular orbital calculations on the entire complex. That is, the entire complex is treated as a single entity and the wave functions obtained from the molecular orbital calculations will have dissymmetry built into them directly (reflecting the symmetry properties of the total molecular Hamiltonian operator). This latter approach has been employed by Schreiner and coworkers[8] and by Strickland and Richardson.[5]

The independent-systems model is expected to be most reliable and useful in treating complexes in which the metal ion–donor group cluster is highly symmetrical and is not inherently chiral. The assumptions and approximations of this model are less valid, however, when the metal ion–donor group cluster is inherently chiral or is of low symmetry. In the latter instances, the second and third approaches outlined above are expected to provide more accurate procedures for calculating the optical activity associated with transitions localized within the metal ion–donor chromophore.

In the present study we examine the optical activity of a series of four-coordinate Cu^{2+} complexes in which the ML_4 ($M = Cu^{2+}$ ion, L = donor groups) cluster may deviate significantly from tetrahedral (T_d) or square-planar (D_{4h}) symmetry. Furthermore, in several of the complexes chosen for study here, the donor atoms belong to ligand groups with extended π-bonding systems and one may expect significant electron delocalization over large parts of the metal complex (metal ion + ligands). For this reason we chose a direct calculational method based on a molecular orbital model for computing rotatory strengths of electronic transitions.

A considerable number of studies on the chiroptical properties of complexes formed between transition metal ions and amino acid, dipeptide, and tripeptide ligands have been reported in the literature.[1a] These studies are of special interest for developing chiroptical spectroscopy as a probe of the structural characteristics of metal ion binding sites in complex biomolecular systems. The spectra–structure relationships discovered for the metal ion–amino acid, –dipeptide, and –tripeptide systems are expected to be at least qualitatively applicable to spectra–structure correlations in metalloenzymes and metal–protein complexes. However, an important difficulty arises in comparing the chiroptical data of these model systems with those obtained for metal ions bound to complex biomolecular systems. In most cases, the metal ion–donor group cluster in the model systems deviates only slightly from a relatively high symmetry and is generally found to be achiral. On the other hand, the donor atoms at metal binding sites in biological macromolecules may be expected to deviate quite significantly from highly symmetrical arrangements in many instances and metal ion–donor group clusters themselves may be chiral. The predominant sources of metal ion optical activity in these latter complex systems may be entirely different from those found to be important in the small model systems, and a common set of spectra–structure relationships may not exist. Whereas configurational dissymmetry, conformational dissymmetry, and/or asymmetric sites in the ligand environment may account for the observed chiroptical properties of the model systems, inherent dissymmetry within the metal ion–donor group cluster may be most important in a large number of metal–biological macromolecular complexes. In the present study we investigate this possibility for Cu^{2+} systems.
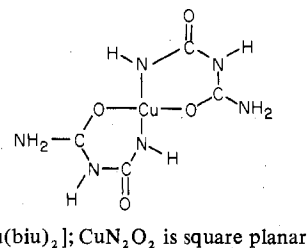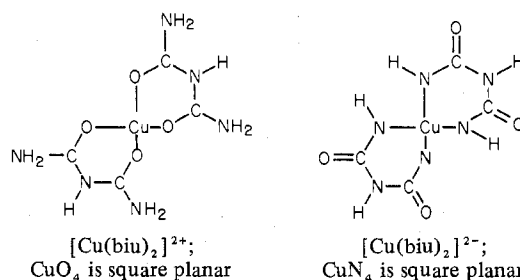
II. Structures

The ligands chosen for this study are all bidentate and each possesses donor atoms or groups which have binding properties

and electronic structural features similar to those expected at metal binding sites in many protein molecules. This choice was guided by our desire to model the chiral binding sites in such systems.

A. Copper(II)–Biuret Complexes. Two types of copper-(II)–biuret complexes have been found to exist in solution and in the solid state. In alkaline solution, bis complexes form in which the Cu^{2+} ion is coordinated in a nearly square-planar configuration by four amide nitrogen atoms from two biuret molecules, each functioning as a dianion due to ionization of two amide hydrogen atoms. These $Cu(biu)_2]^{2-}$ (biu = biuret) complexes have a violet-pink color in solution. In neutral or slightly acidic solution, bis complexes form in which the Cu^{2+} ion is coordinated by four amide oxygen atoms from two biuret molecules, each functioning as a neutral ligand. These $[Cu(biu)_2]^{2+}$ complexes have a blue-green color in solution.

Crystal structure determinations have been reported for both the $[Cu(biu)_2]^{2-}$ and $[Cu(biu)_2]^{2+}$ species.[9] In $[Cu(biu)_2]^{2+}$, the CuO_4 cluster is square planar. However, the complex as a whole is not planar, and within each biuret molecule, the two NH_2CONH residues are not coplanar, the angle between their normals being about 6°. The approximate symmetry of the $[Cu(biu)_2]^{2+}$ complex in crystalline $[Cu(biu)_2]Cl_2$ is C_{2h}, with the two biu ligands related by an inversion operation and a C_2 operation. In crystalline $K_2[Cu(biu)_2]\cdot 4H_2O$, the CuN_4 cluster is square planar. Again, the $[Cu(biu)_2]^{2-}$ complex as a whole is not planar, but deviations from nonplanarity in this system are less than those found for $[Cu(biu)_2]^{2+}$. The approximate symmetry of $[Cu(biu)_2]^{2-}$ in $K_2[Cu(biu)_2]\cdot 4H_2O$ is C_{2h}.

In this study we performed calculations on geometrical isomers of three types of bis(biureto)copper(II) complexes. The three types are (1) $[Cu(biu)_2]^{2+}$ with a CuO_4 coordination cluster, (2) $[Cu(biu)_2]^{2-}$ with a CuN_4 coordination cluster, and (3) $[Cu(biu)_2]$ with a CuN_2O_2 coordination cluster. The reference geometries for each of these types of complexes are depicted.

$[Cu(biu)_2]^{2+}$;
CuO_4 is square planar

$[Cu(biu)_2]^{2-}$;
CuN_4 is square planar

$[Cu(biu)_2]$; CuN_2O_2 is square planar

The symmetries of $[Cu(biu)_2]^{2+}$ and $[Cu(biu)_2]^{2-}$ in their reference geometries were chosen to be C_{2v} (rather than C_{2h}), with the two chelate rings related by a C_2 operation (about a C_2 axis perpendicular to CuO_4 or CuN_4) and a σ_v operation (across a plane which includes Cu and the two –NH chelate bridging groups). The symmetry of $[Cu(biu)_2]$ in its reference geometry was chosen to be C_2 with the chelate rings related by a C_2 operation (about a C_2 axis perpendicular to CuN_2O_2). The structure parameters for $[Cu(biu)_2]^{2+}$ and $[Cu(biu)_2]^{2-}$ in their reference geometries were obtained from crystal structure data (determined by x-ray diffraction techniques),

and the structure parameters for [Cu(biu)$_2$] were adapted from those known for [Cu(biu)$_2$]$^{2+}$ and [Cu(biu)$_2$]$^{2-}$.

Additional geometrical isomers of [Cu(biu)$_2$]$^{2+}$, [Cu(biu)$_2$]$^{2-}$, and [Cu(biu)$_2$] were generated by rotating one of the chelate rings about a dihedral axis of the coordination cluster while holding the other chelate ring stationary. This operation is depicted as
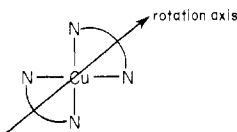
Bond angles and bond distances within each chelate ring, as well as the chelate bite angles, were held constant in performing this operation. The angle by which the one chelate ring·is rotated is denoted by θ. For $\theta \neq 0$ and 180°, the [Cu(biu)$_2$]$^{2+}$ and [Cu(biu)$_2$]$^{2-}$ complexes possess exact C_2 symmetry; at $\theta = 0°$ (reference geometry) each of these complexes has C_{2v} symmetry and at $\theta = 180°$ each complex has C_{2h} symmetry. [Cu(biu)$_2$] has C_2 symmetry for all values of θ.

In addition to making calculations on the bis complexes of biuret, we also performed calculations on a number of mono complexes in which one biuret ligand is replaced either by two water molecules or by two hydroxyl ions.

B. Copper(II)–Glycine Complexes. We performed calculations on a series of geometrical isomers of bis(glycinato)copper(II). As a reference geometry we chose the trans structure

CuN$_2$O$_2$ is planar
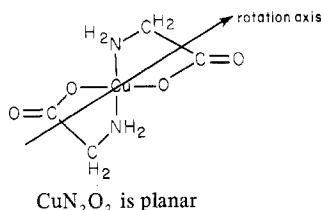
The geometries of the chelate rings were generated from crystal structure data on bis(glycinato)copper(II) monohydrate.[9] In our reference structure each nonplanar chelate ring has the same chirality and the two chelate rings are related by a C_2 operation (about a C_2 perpendicular to the CuN$_2$O$_2$ coordination cluster). The trans reference structure has, then, exact C_2 point group symmetry. Geometrical isomers of [Cu(gly)$_2$] were generated by rotating one of the chelate rings about an axis which bisects the two rings. For all values of the rotation angle θ, the [Cu(gly)$_2$] complex retains exact C_2 symmetry.

C. Copper(II)–Glycinamide Complexes. Calculations were also performed on a series of bis complexes formed by Cu^{2+} and two CH$_2$(NH$_2$)CONH$_2$ ligands. The structures for these [Cu(glya)$_2$] complexes were adapted from those generated for [Cu(gly)$_2$] by replacing a carboxyl group on each ligand with a deprotonated amide group (–CONH$^-$).

D. Copper(II)–(S)-Alanine Complexes and –(S)-Alaninamide Complexes. Calculations were performed on a series of [Cu(S-ala)$_2$] and [Cu(S-alaa)$_2$] structures which differ from the [Cu(gly)$_2$] and [Cu(glya)$_2$] structures, respectively, only with respect to –CH$_3$ substitution at the α-carbon atom of each ligand.

III. Theoretical Model

A. General Data. In this study we employ the direct calculational approach to compute the chiroptical properties of the d–d and lowest lying charge-transfer (CT) transitions of the Cu^{2+} systems. That is, the rotatory strengths

$$R_{ij} = \text{Im}\langle \psi_i | \hat{\mu} | \psi_j \rangle \cdot \langle \psi_j | \hat{m} | \psi_i \rangle \tag{1}$$

where $\hat{\mu}$ is the electric dipole operator and $\hat{m}$ is the magnetic dipole operator, are calculated using wave functions which are obtained as approximate eigenfunctions of the *complete* (*but nonrelativistic*) electronic Schrödinger equation for each complex. The shortcomings of this approach reside in the rather serious approximations one must make in solving the electronic Schrödinger equation for such large systems as are examined here and especially in constructing wave functions for the spectroscopic excited states. Despite these obvious shortcomings, this approach is much preferred over an independent-systems or perturbative model for systems in which electron delocalization beyond the metal ion–donor atom cluster is expected to be significant and in which the chromophoric unit is not localized at a center of high symmetry.

In addition to rotatory strengths, we also calculate electric dipole strengths of the d–d and low-lying CT transitions

$$D_{ij} = |\langle \psi_i | \hat{\mu} | \psi_j \rangle|^2 \tag{2}$$

B. Electronic Wave Functions. Ground-state wave functions are calculated using a modified Wolfsberg–Helmholz or extended Hückel molecular orbital model. The general procedures we use in carrying out calculations on this model have been described elsewhere and will not be discussed further here (see ref 5, section II.A.1). The atomic orbital basis set employed in our calculations includes (1) 3d, 4s, and 4p orbitals on Cu^{2+}, (2) 2s and 2p orbitals on each C, N, and O atom, and (3) a 1s orbital on each H atom. The single-ζ Slater-type orbitals (STO) of Clementi and Raimondi[10] were chosen for the C, N, and O atoms. For the H atoms, we used a Slater-type 1s orbital with $\zeta = 1.2$. The metal ion basis set consisted of single-ζ 4s and 4p orbitals and double-ζ 3d orbitals.[11]

Excited-state wave functions are constructed in the virtual orbital approximation by promoting an electron from an occupied molecular orbital to an unoccupied (or virtual) orbital.

C. Electric and Magnetic Dipole Transition Moments. To calculate electronic rotatory strengths (eq 1) and dipole strengths (eq 2) both electric and magnetic dipole transition integrals are required. The electric dipole transition integrals are calculated in the dipole velocity representation and then transformed to the dipole length representation by the relationship

$$\langle \psi_i | \partial/\partial q | \psi_j \rangle = \frac{m^2 (E_j - E_i)}{\hbar^2} \langle \psi_i | q | \psi_j \rangle \tag{3}$$

where $q = x, y,$ or z (electron positional coordinate). All one-, two-, and three-center terms in the electric dipole velocity and angular momentum integrals are included in computing the $\langle \psi_i | \hat{\mu} | \psi_j \rangle$ and $\langle \psi_i | \hat{m} | \psi_j \rangle$ matrix elements. The electric and magnetic dipole transition integrals, dipole strengths, rotatory strengths, oscillator strengths, and dissymmetry factors ($4R_{ij}/D_{ij}$) are calculated using a program (ROTSTR) previously employed in computing chiroptical properties of nonmetal systems and extended in the present study to handle 4s, 4p, and 3d metal orbitals.[12]

IV. Results

A. Copper(II)–Biuret Complexes (d–d Transitions). The optical properties computed for the four lowest energy transitions of various copper(II)–biuret complexes are listed in Tables I–IV. On our model, the four lowest energy transitions in each of these systems are essentially d–d excitations localized on the metal ion. In the near-planar structures ($\theta \approx 0$ or 180°) of [Cu(biu)$_2$]$^{2+}$ the energy ordering of the Cu^{2+} 3d orbitals is 3d$_{x^2-y^2}$ > 3d$_{xy}$ > (3d$_{xz}$, 3d$_{yz}$) > 3d$_{z^2}$, and the 3d$_{xy}$ and 3d$_{z^2}$ orbitals are mixed extensively. In this complex, all four donor atoms are carbonyl oxygens. The energy ordering of the Cu^{2+} 3d orbitals in the near-planar

Table I. Computed Optical Properties of the Four Lowest Transitions in [Cu(biu)₂]²⁺

θ, deg	Transition (symmetry)ᵃ	ΔE, eV	D, D²	$10^{40}R$, cgsu	$\lvert G \rvert = \lvert 4R/D \rvert$	$10^{40}R_{net}$,ᵇ cgsu
0	1 (A)	2.14	0.0014	0	0	0
	2 (B)	2.18	0.0026	0	0	
	3 (B)	2.19	0.0361	0	0	
	4 (A)	2.26	0.0049	0	0	
6	1 (A)	2.17	0.0030	−6.25	0.7736	6.77
	2 (B)	2.20	0.0058	4.89	0.3124	
	3 (B)	2.22	0.0482	2.22	0.0171	
	4 (A)	2.28	0.0062	5.91	0.3502	
15	1 (A)	2.12	0.0168	−14.80	0.3768	16.12
	2 (B)	2.12	0.0800	17.47	0.0809	
	3 (B)	2.16	0.0464	−0.33	0.0026	
	4 (A)	2.23	0.0326	13.48	0.1536	
30	1 (B)	1.86	0.3208	32.99	0.0381	24.88
	2 (A)	1.95	0.0450	−24.32	0.2009	
	3 (B)	1.97	0.0270	−2.60	0.0358	
	4 (A)	2.05	0.0634	18.81	0.1101	
60	1 (B)	1.01	0.8450	48.01	0.0211	35.50
	2 (B)	1.43	0.0096	−5.51	0.2111	
	3 (A)	1.46	0.0164	−15.23	0.3465	
	4 (A)	1.52	0.0124	8.23	0.2451	
90	1 (B)					−51.19
	2 (B)	0.88	0.0444	−13.19	0.1101	
	3 (A)	0.93	0.1316	46.51	0.1311	
	4 (A)	0.98	1.3656	−84.51	0.0226	

ᵃ Symmetry with respect to the C_2 axis of the complex.
ᵇ $R_{net} = R_1 + R_2 + R_3 + R_4$.

Table II. Computed Optical Properties of the Four Lowest Transitions in [Cu(biu)₂]²⁻

θ, deg	Transition (symmetry)ᵃ	ΔE, eV	D, D²	$10^{40}R$, cgsu	$\lvert G \rvert = \lvert 4R/D \rvert$	$10^{40}R_{net}$,ᵇ cgsu
0	1 (B)	2.67	0.0046	0	0	0
	2 (B)	2.92	0.0022	0	0	
	3 (A)	3.02	0.0003	0	0	
	4 (A)	3.19	0.0004	0	0	
6	1 (B)	2.66	0.0303	−4.91	0.0647	−3.70
	2 (B)	2.92	0.0215	5.46	0.1015	
	3 (A)	3.03	0.0019	−2.95	0.6144	
	4 (A)	3.17	0.0030	−1.30	0.1734	
15	1 (B)	2.46	0.0814	−6.20	0.0305	−16.60
	2 (B)	2.63	0.0522	8.15	0.0625	
	3 (A)	2.91	0.0280	−14.40	0.2057	
	4 (A)	3.01	0.0120	−4.15	0.1383	
30	1 (B)	2.17	0.0187	−11.06	0.0236	−24.08
	2 (B)	2.52	0.2229	17.22	0.0309	
	3 (A)	2.70	0.2284	−21.18	0.0371	
	4 (A)	2.71	0.0153	−9.06	0.2367	
60	1 (B)	1.15	0.3038	−12.15	0.0160	−53.81
	2 (B)	1.83	0.3200	20.80	0.0260	
	3 (A)	1.87	0.0352	−6.67	0.0757	
	4 (A)	1.98	0.4959	−55.79	0.0450	
90	1 (B)					−86.99
	2 (A)	1.16	0.6634	−33.89	0.0189	
	3 (B)	1.19	0.0136	4.44	0.1215	
	4 (A)	1.34	0.4634	−57.54	0.0461	

ᵃ Symmetry with respect to the C_2 axis of the complex.
ᵇ $R_{net} = R_1 + R_2 + R_3 + R_4$.

Table III. Computed Optical Properties of the Four Lowest Transitions in [Cu(biu)₂]

θ, deg	Transition (symmetry)ᵃ	ΔE, eV	D, D²	$10^{40}R$, cgsu	$\lvert G \rvert = \lvert 4R/D \rvert$	$10^{40}R_{net}$,ᵇ cgsu
0 (trans)	1 (B)	2.29	0.1668	−16.27	0.0362	−7.63
	2 (A)	2.60	0.0048	6.04	0.4735	
	3 (B)	2.64	0.0044	−0.85	0.0707	
	4 (A)	2.71	0.0014	3.45	0.9464	
180 (cis)	1 (B)	2.44	0.4622	−2.53	0.0020	−10.94
	2 (A)	2.57	0.0464	−12.77	0.1052	
	3 (B)	2.65	0.0844	2.40	0.0105	
	4 (B)	2.76	0.0094	1.96	0.0776	
15	1 (B)	2.20	0.1240	−14.18	0.0424	−13.47
	2 (A)	2.52	0.0280	−12.80	0.1703	
	3 (B)	2.56	0.0940	4.19	0.0165	
	4 (A)	2.63	0.0078	9.32	0.4388	
−15	1 (B)	2.20	0.2572	−16.86	0.0243	2.97
	2 (A)	2.54	0.0918	28.86	0.1166	
	3 (B)	2.54	0.0310	−4.64	0.0555	
	4 (A)	2.62	0.0028	−4.39	0.5889	
30	1 (B)	1.97	0.2126	−3.45	0.0065	−39.77
	2 (A)	2.12	0.0291	−8.62	0.1185	
	3 (B)	2.19	0.0810	3.92	0.0194	
	4 (A)	2.30	0.0112	−31.62	1.1292	
60	1 (B)	1.11	0.5030	9.87	0.0073	−67.62
	2 (B)	1.71	0.6094	−0.37	0.0002	
	3 (A)	1.75	0.0400	3.41	0.0317	
	4 (A)	1.82	0.3802	−80.53	0.0785	

ᵃ Symmetry with respect to the C_2 axis of the complex.
ᵇ $R_{net} = R_1 + R_2 + R_3 + R_4$.

Table IV. Computed Optical Properties of the Four Lowest Transitions in [Cu(biu)(OH)₂]⁻ and in [Cu(biu)(H₂O)₂]⁺

θ, deg	Transition	ΔE, eV	D, D²	$10^{40}R$, cgsu	$\lvert G \rvert = \lvert 4R/D \rvert$	$10^{40}R_{net}$,ᵃ cgsu
			[Cu(biu)(H₂O)₂]⁺			
0	1	1.60	0.5734	−9.78	0.0064	−6.16
	2	1.77	0.0226	4.22	0.0691	
	3	1.79	0.1876	−5.10	0.0101	
	4	1.86	0.4662	4.50	0.0036	
60	1	0.89	2.4412	10.05	0.0011	−57.03
	2	1.23	0.8706	14.27	0.0061	
	3	1.29	0.8278	−30.53	0.0137	
	4	1.37	0.2340	−50.82	0.0565	
90	1					−10.73
	2	0.98	0.8352	1.62	0.0007	
	3	1.00	5.1600	7.28	0.0005	
	4	1.11	0.4252	−19.63	0.0172	
			[Cu(biu)(OH)₂]⁻			
0	1	1.38	1.4882	11.30	0.0026	−9.39
	2	1.49	0.2306	−18.40	0.0296	
	3	1.55	0.0346	1.26	0.0135	
	4	1.61	0.5654	−3.55	0.0024	
60	1	0.76	2.2212	8.61	0.0016	−58.04
	2	1.14	0.9641	−24.21	0.0100	
	3	1.22	1.2141	−6.24	0.0021	
	4	1.33	0.3614	−36.20	0.0401	

ᵃ $R_{net} = R_1 + R_2 + R_3 + R_4$.

structures of [Cu(biu)₂]²⁻ was computed to be $3d_{x^2-y^2} > (3d_{xz},$ $3d_{yz}) > 3d_{xy} > 3d_{z^2}$, where again the $3d_{xy}$ and $3d_{z^2}$ orbitals are extensively mixed. In this complex, all four donor atoms are amide nitrogens.

In the trans (θ = 0°) isomer of [Cu(biu)₂], the energy ordering of the Cu²⁺ 3d orbitals was computed to be $3d_{x^2-y^2} > 3d_{yz} > (3d_{z^2}, 3d_{xy}) > 3d_{xz} > (3d_{z^2}, 3d_{xy})$, where $(3d_{z^2}, 3d_{xy})$ denotes levels in which the $3d_{z^2}$ and $3d_{xy}$ orbitals are present in nearly equal amounts. In this structure, the amide nitrogen

donor atoms lie along the y axis and the carbonyl oxygen donor atoms lie along the x axis. For the cis (θ = 180°) isomer of [Cu(biu)₂], the energy ordering of the 3d orbitals was found to be $3d_{x^2-y^2} > (3d_{xz}, 3d_{yz}) > 3d_{z^2} > 3d_{xy}$.

The energy ordering of the Cu²⁺ 3d orbitals in [Cu(biu)(H₂O)₂]⁺ at θ = 0° (near-planar structure) is $3d_{x^2-y^2} > 3d_{yz} > 3d_{xz} > 3d_{z^2} > 3d_{xy}$, whereas in the [Cu(biu)(OH)₂]⁻ complex at θ = 0° the energy ordering is $3d_{x^2-y^2} > 3d_{yz} > 3d_{xy} > 3d_{xz} > 3d_{z^2}$. In these structures, the amide nitrogen donor atom lies along the y axis.

B. Copper(II)–Biuret Complexes (CT Transitions). The optical properties computed for the three lowest energy charge-transfer transitions are listed in Table V for several

Table V. Computed Optical Properties of the Three Lowest Energy Charge-Transfer Transitions in Copper(II)–Biuret Complexes

θ, deg	Transition (symmetry)^a	ΔE, eV	D, D^2	$10^{40}R$, cgsu	$\lvert G\rvert = \lvert 4R/D\rvert$	10^{40}-R_{net},^{b} cgsu
			$[Cu(biu)_2]^{2+}$			
0	5 (B)	2.94	1.0126	0	0	0
	6 (A)	2.96	0	0	0	
	7 (B)	3.71	17.2614	0	0	
60	5 (B)	2.90	1.0818	−0.58	0.0002	−14.12
	6 (A)	2.95	0.0001	0.02	1.9081	
	7 (B)	3.65	16.1026	−13.56	0.0003	
15	5 (B)	2.85	1.1278	−1.51	0.0005	−33.65
	6 (A)	2.90	0.0002	0.03	1.0126	
	7 (B)	3.61	15.9676	−32.17	0.0008	
			$[Cu(biu)_2]^{2-}$			
0	5 (B)	4.45	0.0330	0	0	0
	6 (A)	4.69	0.2304	0	0	
	7 (A)	4.79	0	0	0	
6	5 (B)	4.44	0.1452	13.28	0.0339	·11.18
	6 (A)	4.63	0.0614	−0.91	0.0055	
	7 (A)	4.80	0.2210	−1.19	0.0020	
15	5 (B)	4.43	0.0928	28.15	0.1213	15.08
	6 (A)	4.58	0.0417	−0.96	0.0092	
	7 (A)	4.84	0.3642	−12.11	0.0133	
			$[Cu(biu)_2]$			
0 (trans)	5 (A)	3.28	0.0678	5.88	0.0322	7.10
	6 (B)	3.40	0.6094	19.96	0.0122	
	7 (B)	4.15	3.6350	−18.74	0.0019	
180 (cis)	5 (B)	3.32	0.2250	17.35	0.0308	7.71
	6 (A)	3.44	0.4780	11.62	0.0097	
	7 (A)	4.16	1.8294	−21.26	0.0046	
15	5 (A)	3.22	0.0512	3.65	0.0285	20.00
	6 (B)	3.30	0.8574	25.36	0.0118	
	7 (B)	4.06	3.3386	−9.01	0.0011	
−15	5 (A)	3.21	0.0454	5.90	0.0520	−9.97
	6 (B)	3.33	0.5222	13.41	0.0102	
	7 (B)	4.10	4.0010	−29.28	0.0029	

^{a} Symmetry with respect to the C_2 axis of the complex.
^{b} $R_{net} = R_5 + R_6 + R_7$.

Table VI. Computed Optical Properties of the Four Lowest Transitions in $[Cu(gly)_2]$

θ, deg	Transition (symmetry)^a	ΔE, eV	D, D^2	$10^{40}R$, cgsu	$\lvert G\rvert = \lvert 4R/D\rvert$	10^{40}-R_{net},^{b} cgsu
0 (trans)	1 (A)	2.18	0.0012	0.45	0.1481	6.47
	2 (A)	2.64	0.0004	1.94	2.2506	
	3 (B)	2.66	0.1900	−21.00	0.0410	
	4 (B)	2.77	0.3722	25.08	0.0250	
15	1 (A)	2.09	0.0822	−·7.00	0.0316	55.39
	2 (B)	2.53	0.2541	−30.29	0.0442	
	3 (A)	2.55	0.0249	23.97	0.3572	
	4 (B)	2.60	1.2621	68.71	0.0202	
−15	1 (A)	2.08	0.1097	6.91	0.0009	−63.79
	2 (B)	2.53	0.0779	−19.21	0.0007	
	3 (A)	2.54	0.0173	−20.30	0.0002	
	4 (B)	2.61	0.9808	−31.19	0.0097	
180 (cis)	1 (A)	2.20	4.0554	−3.57	0.0004	1.32
	2 (B)	2.68	0.0123	2.46	0.0800	
	3 (B)	2.73	0.0260	4.39	0.0675	
	4 (A)	2.76	0.0005	−1.96	0	
165	1 (B)	2.09	4.1973	4.19	0.0004	−13.78
	2 (B)	2.58	0.0466	−22.01	0.1889	
	3 (B)	2.60	0.0093	−1.04	0.0447	
	4 (A)	2.63	0.0035	5.08	0	
195	1 (B)	2.08	4.5216	−·5.62	0.0005	6.98
	2 (B)	2.59	0.0572	15.61	0.1092	
	3 (B)	2.62	0.0181	−11.20	0.2435	
	4 (A)	2.63	0.0460	8.19	0.0712	

^{a} Symmetry with respect to the C_2 axis of the complex.
^{b} $R_{net} = R_1 + R_2 + R_3 + R_4$.

Table VII. Computed Optical Properties of the Four Lowest Transitions in $[Cu(glya)_2]$

θ, deg	Transition (symmetry)^a	ΔE, eV	D, D^2	$10^{40}R$, cgsu	$\lvert G\rvert = \lvert 4R/D\rvert$	10^{40}-R_{net},^{b} cgsu
0 (trans)	1 (B)	2.87	0.1178	−10.30	0.0350	6.02
	2 (A)	2.89	0.0178	4.35	0.0903	
	3 (A)	3.13	0.0034	5.32	0.5842	
	4 (B)	3.25	0.0308	6.65	0.0801	
180 (cis)	1 (B)	2.82	4.3208	−14.77	0.0014	2.36
	2 (B)	2.99	0.1822	15.93	0.0324	
	3 (B)	3.13	0.0594	6.37	0.0429	
	4 (A)	3.15	0.0086	−5.17	0.2238	

^{a} Symmetry with respect to the C_2 axis of the complex.
^{b} $R_{net} = R_1 + R_2 + R_3 + R_4$.

Table VIII. Computed Optical Properties of the Four Lowest Transitions in $[Cu(gly)_2(H_2O)_2]$

θ, deg	Transition	ΔE, eV	D, D^2	$10^{40}R$, cgsu	$\lvert G\rvert = \lvert 4R/D\rvert$	10^{40}-R_{net},^{a} cgsu
0	1	1.99	0.0014	0.04	0.0108	·8.88
	2	2.58	0.0006	2.29	1.6919	
	3	2.65	0.1970	−21.34	0.0402	
	4	2.76	0.2356	27.84	0.0439	
180	1	2.09	0.2900	−0.01	0	2.59
	2	2.56	0.0846	1.04	0.0049	
	3	2.73	0.0315	3.98	0.0505	
	4	2.78	0.0009	−2.42	0.1076	

^{a} $R_{net} = R_1 + R_2 + R_3 + R_4$.

of the copper(II)–biuret structures. In each of the [Cu(biu)2]$^{2+}$ structures, these three transitions are of the ligand → metal charge-transfer type with the acceptor orbital being metal 3d$_{x^2-y^2}$ and the donor orbitals being ligand 2p$_\pi$ (out of plane). In the near-planar [Cu(biu)2]$^{2-}$ structures, the first and third charge-transfer transitions are ligand (2p$_\pi$) → metal (3d$_{x^2-y^2}$) and the second charge-transfer transition is ligand (2p$_\sigma$) → metal (3d$_{x^2-y^2}$). In the near-planar [Cu(biu)2] structures, the first two (lowest energy) charge-transfer transitions are ligand (2p$_\pi$) → metal (3d$_{x^2-y^2}$) and the third transition is ligand (2p$_\sigma$) → metal (3d$_{x^2-y^2}$).

C. Copper(II)–Glycine and –Glycinamide Complexes (d–d Transitions). The optical properties computed for the four lowest energy transitions of various copper(II)–glycine and copper(II)–glycinamide complexes are displayed in Tables VI–VIII. The four lowest energy transitions in each of these systems are computed to be essentially of the d–d ligand field type localized on the metal ion. In the [Cu(gly)2(H2O)2] structures, the water molecules occupy axial positions with Cu–OH2 bond lengths of 2.50 Å. The energy ordering of the Cu^{2+} 3d orbitals in the near-planar trans ($\theta = 0°$) glycine complexes was found to be 3d$_{x^2-y^2}$ > 3d$_{z^2}$ > 3d$_{xy}$ > 3d$_{xz}$ > 3d$_{yz}$ (the carboxyl oxygen donor atoms lie along the x axis). In the cis ($\theta = 180°$) glycine structures, the 3d energy ordering is 3d$_{x^2-y^2}$ > 3d$_{z^2}$ > 3d$_{xy}$ > (3d$_{xz}$, 3d$_{yz}$). The 3d energy ordering computed for the trans ($\theta = 0°$) glycinamide complex [Cu(glya)2] is 3d$_{x^2-y^2}$ > 3d$_{xz}$ > 3d$_{z^2}$ > 3d$_{xy}$ > 3d$_{yz}$ (the amide nitrogen donor atoms are located along the x axis), and the

computed energy ordering for the cis ($\theta = 180°$) glycinamide complex is 3d$_{x^2-y^2}$ > 3d$_{z^2}$ > (3d$_{xz}$, 3d$_{yz}$) > 3d$_{xy}$ > (3d$_{xz}$, 3d$_{yz}$).

D. Copper(II)–Glycine and –Glycinamide Complexes (CT Transitions). The optical properties computed for the three lowest energy charge-transfer transitions are listed in Table IX for several copper(II)–glycine and copper(II)–glycinamide complexes. These transitions are of the ligand → metal charge-transfer type for each structure. The first and third CT transitions involve ligand (2p$_\pi$) → metal (3d$_{x^2-y^2}$) exci-

Table IX. Computed Optical Properties of the Three Lowest Energy Charge-Transfer Transitions in Copper(II)–Glycine and –Glycinamide Complexes

θ, deg	Transition (symmetry)^a	ΔE, eV	D, D^2	$10^{40}R$, cgsu	$\|G\| = \|4R/D\|$	$10^{40}R_{net}$,^{b} cgsu
			Cu[gly]$_2$			
0 (trans)	5 (B)	3.01	5.5760	−4.12	0.0003	2.48
	6 (A)	3.28	0	0.46		
	7 (B)	4.62	3.0451	6.14	0.0007	
180 (cis)	5 (A)	3.02	0.0124	3.56	0.1060	4.46
	6 (B)	3.37	3.7006	−1.73	0.0002	
	7 (A)	4.56	2.5104	2.63	0.0004	
			[Cu(gly)$_2$(H$_2$O)$_2$]			
0 (trans)	5 (B)	2.98	5.5961	−6.86	0.0005	5.85
	6 (A)	3.24	0	0.85		
	7 (B)	4.60	3.1108	11.86	0.0014	
180 (cis)	5 (A)	2.99	0.0286	2.92	0.0378	9.00
	6 (B)	3.06	0.6124	−0.29	0.0002	
	7 (A)	3.07	2.2838	6.37	0.0010	
			[Cu(glya)$_2$]			
0 (trans)	5 (B)	3.62	10.5196	4.35	0.0002	55.96
	6 (A)	3.94	0.0022	−4.92	0.8165	
	7 (B)	4.83	1.9570	56.53	0.0107	
180 (cis)	5 (A)	3.75	0.0494	2.93	0.0220	23.42
	6 (B)	3.85	8.2619	4.47	0.0002	
	7 (B)	4.71	0.2976	16.02	0.0200	

^{a} Symmetry with respect to the C_2 axis of the complex.
^{b} $R_{net} = R_5 + R_6 + R_7$.

Table X. Computed Optical Properties of the Seven Lowest Energy Transitions in *trans*-[Cu(S-ala)$_2$] Structures

Transition (symmetry)^a	ΔE, eV	D, D^2	$10^{40}R$, cgsu	$\|G\| = \|4R/D\|$	$10^{40}R_{net}$, cgsu
		α-Methyl Substituent Axial			
1 (A)	2.09	0.0617	1.01	0.0065	
2 (A)	2.59	0.0059	−5.91	0.4006	
3 (B)	2.75	0.1640	−14.35	0.0350	−32.47
4 (B)	2.80	0.2280	−13.22	0.0232	
5 (B)	3.01	4.4398	−40.43	0.0036	
6 (A)	3.13	0.0538	18.77	0.1396	−14.11
7 (B)	3.89	0.7582	7.55	0.0040	
		α-Methyl Substituent Equatorial			
1 (A)	1.98	0.0184	2.67	0.0580	
2 (A)	2.49	0.0151	−18.33	0.4856	
3 (B)	2.85	0.1725	−19.74	0.0458	−44.00
4 (B)	2.91	0.1618	−8.60	0.0213	
5 (B)	3.03	7.7063	−54.01	0.0028	
6 (A)	3.31	0.4276	22.92	0.0214	−31.16
7 (B)	3.86	2.8029	−0.65	0.0001	

^{a} Symmetry with respect to the C_2 axis of the complex.

Table XI. Computed Optical Properties of the Seven Lowest Energy Transitions in *cis*-[Cu(S-ala)$_2$] Structures

Transition (symmetry)^a	ΔE, eV	D, D^2	$10^{40}R$, cgsu	$\|G\| = \|4R/D\|$	$10^{40}R_{net}$, cgsu
		α-Methyl Substituent Axial			
1 (B)	2.24	1.6199	0.14		
2 (B)	2.66	0.0744	1.49	0.0080	
3 (B)	2.81	0.0937	6.45	0.0275	19.94
4 (A)	2.84	0.0742	11.86	0.0639	
5 (A)	2.92	7.6411	10.84	0.0006	
6 (B)	3.27	0	57.17		65.71
7 (B)	3.96	3.8927	−2.30	0.0002	
		α-Methyl Substituent Equatorial			
1 (B)	2.31	0.5562	−15.87	0.0114	
2 (B)	2.78	0.0094	8.04	0.3421	2.24
3 (B)	2.93	0.0140	6.64	0.1897	
4 (A)	2.98	0.0160	3.43	0.0858	
5 (A)	3.09	0.7670	11.83	0.0062	
6 (B)	3.42	4.5866	59.55	0.0052	17.78
7 (B)	4.01	2.5619	−53.60	0.0084	

^{a} Symmetry with respect to the C_2 axis of complex.

Table XII. Computed Optical Properties of the Seven Lowest Energy Transitions in *trans*-[Cu(S-alaa)$_2$] Structures

Transition (symmetry)^a	ΔE, eV	D, D^2	$10^{40}R$, cgsu	$\|G\| = \|4R/D\|$	$10^{40}R_{net}$, cgsu
		α-Methyl Substituent Axial			
1 (B)	2.59	0.1120	−11.61	0.0415	
2 (A)	2.73	0.0190	−3.61	0.0760	−59.03
3 (A)	2.92	0.0088	−46.22	2.1009	
4 (B)	3.01	0.0319	2.41	0.0302	
5 (B)	3.94	9.7441	49.44	0.0020	
6 (A)	4.18	0.0366	12.78	0.1397	39.92
7 (B)	4.99	2.8748	−22.30	0.0031	
		α-Methyl Substituent Equatorial			
1 (B)	2.47	0.1261	−9.64	0.0306	
2 (A)	2.64	0.0242	−5.94	0.0981	−65.46
3 (A)	2.86	0.0108	−51.87	1.9211	
4 (B)	2.96	0.0264	1.99	0.0305	
5 (B)	3.98	8.6119	58.94	0.0027	
6 (A)	4.02	0.0162	8.44	0.2083	35.70
7 (B)	5.06	3.6417	−31.68	0.0035	

^{a} Symmetry with respect to the C_2 axis of the complex.

Chart I

	x, Å	y, Å	z, Å
Cu^{2+}	0	0	0
O$^-$	1.9503	0.0817	0
C(carbonyl)	2.4537	1.2619	0
C$_\alpha$	1.4928	2.4312	0.1170
N	0.0838	2.0002	0
O(carbonyl)	3.6652	1.4842	−0.0894

Chart II

	x, Å	y, Å	z, Å
Cu^{2+}	0	0	0
O$^-$	1.9503	0.0817	0
C(carbonyl)	2.4537	1.2619	0
C$_\alpha$	1.4928	2.4312	−0.1170
N	0.0838	2.0002	0
O(carbonyl)	3.6652	1.4842	0.0894

tations, whereas the second CT transition is due to a ligand (2p$_\sigma$) → metal (3d$_{x^2-y^2}$) process.

E. Copper(II)–Alanine Complexes. Optical properties computed for the seven lowest energy transitions in several [Cu(S-ala)$_2$] structures are listed in Tables X and XI. The assignments of these transitions in the *trans*-[Cu(S-ala)$_2$] structures (Table X) are identical with those given for the trans (θ = 0°) isomer of [Cu(gly)$_2$]. Likewise, the assignments of the seven lowest energy transitions in the *cis*-[Cu(S-ala)$_2$] structures (Table XI) are identical with those given for the cis (θ = 180°) isomer of [Cu(gly)$_2$].

The chelate ring geometries of the *cis*- and *trans*-[Cu(gly)$_2$] complexes examined in this study are identical. Atomic positional coordinates for the ring atoms plus the carbonyl oxygen atom are listed in Chart I for the copper(II)–glycine chelate system. This ring geometry was also used for the [Cu(S-ala)$_2$] complexes in which the α-methyl substituent is

disposed *axial* to the chelate ring. For the [Cu(S-ala)$_2$] complexes in which the α-methyl substituent is disposed *equatorial* to the chelate ring, the atomic positional coordinates of the ring atoms plus the carbonyl oxygen are given in Chart II. The chelate rings in the [Cu(gly)$_2$] and [Cu(S-ala)$_2$] (CH$_3$ axial) complexes have identical conformations, whereas the chelate ring conformation in the [Cu(S-ala)$_2$] (CH$_3$ equatorial) complexes is enantiomeric to that found in [Cu(gly)$_2$].

F. Copper(II)–Alaninamide Complexes. Optical properties

computed for the seven lowest energy transitions in two isomers of *trans*-[Cu(S-alaa)₂] are listed in Table XII. The assignments of these transitions in *trans*-[Cu(S-alaa)₂] are identical with those given for the trans ($\theta = 0°$) isomer of [Cu(glya)₂]. The chelate ring conformations in *trans*-[Cu(S-alaa)₂] (CH₃ axial), *trans*-[Cu(S-ala)₂] (CH₃ axial), [Cu(gly)₂], and [Cu(glya)₂] are the same and are enantiomeric to those in *trans*-[Cu(S-alaa)₂] (CH₃ equatorial) and in *trans*-[Cu(S-ala)₂] (CH₃ equatorial).

V. Discussion

A. Copper(II)–Biuret Complexes. The sources of chirality in the [Cu(biu)₂]²⁺ and [Cu(biu)₂]²⁻ systems are identical. In each of the isomers examined here the individual chelate rings retain a plane of symmetry and the metal ion–donor atom cluster possesses either D_{4h} or D_{2d} symmetry. If we restrict our definition of the chromophoric group to just the metal ion–donor atom cluster, then these structures become optically active by virtue of configurational dissymmetry alone. If we extend the chromophoric group description to include the amide moieties in the metal ion–donor group cluster, then the chromophore possesses inherent dissymmetry for all values of $\theta \neq 0, 180°$.

Both the carbonyl oxygen atoms in [Cu(biu)₂]²⁺ and the amide nitrogen atoms in [Cu(biu)₂]²⁻ exhibit strong π-bonding interactions with Cu²⁺. However, whereas the *in-plane* metal–ligand π interactions dominate over the *out-of-plane* metal–ligand π interactions in [Cu(biu)₂]²⁺, the *out-of-plane* metal–ligand π interactions dominate in [Cu(biu)₂]²⁻. This results in different relative orderings of the 3d₍π₎ Cu²⁺ orbitals in the two types of complexes. In the absence of five- and six-coordination or axial perturbations, the 3d₍z²₎ orbital lies lowest in each of the near-planar structures of these complexes and the 3d₍x²−y²₎ orbital lies highest. The d–d transitions of the [Cu(biu)₂]²⁺ complex lie to the red of the d–d transitions in [Cu(biu)₂]²⁻. An especially interesting result is the opposition in signs of the net d–d rotatory strengths computed for the [Cu(biu)₂]²⁺ and [Cu(biu)₂]²⁻ complexes for all values of θ except those within ~±10° of $\theta = 90$. This opposition of signs also holds for the net rotatory strengths computed for the three lowest energy charge-transfer transitions in [Cu(biu)₂]²⁺ and [Cu(biu)₂]²⁻. The configurational chiralities of these two complexes are identical for specified values of θ. This suggests that the signs of the net rotatory strengths (or the rotatory strengths of individual transitions) cannot be related simply to configurational chirality without taking into consideration the detailed nature of the donor groups or of the extended chromophore.

In the [Cu(biu)₂] structures, the individual chelate rings are chiral so that these complexes exhibit optical activity for all values of θ. In these systems the amide nitrogen donors again interact strongly with the metal ion through out-of-plane π interactions, whereas the Cu–O linkages involve strong in-plane π interactions. The energy orderings of the 3d orbitals in these complexes differ from those in [Cu(biu)₂]²⁺ and [Cu(biu)₂]²⁻, as discussed in section IV.A.

In all three bis(biuret) complexes examined in this study, a strong correlation between the signs and relative magnitudes of the *net* rotatory strengths (d–d and low-lying CT) and the structure parameter θ has been found. As is evident from the data presented in Tables I–III and V, simple correlations between θ and the rotatory strengths of individual transitions are not so apparent. The relative energy orderings and the mixings of d–d states and CT states are exceedingly sensitive to variations in θ. This leads to ambiguities in the systematic assignment of transitions to specific orbital excitations as θ is varied and to considerable difficulties in making spectra–structure correlations based on individual CD or absorption bands.

The orbital occupation numbers calculated for the 4s, 4p, and 3d₍x²−y²₎ metal orbitals in the ground state of the near-planar [Cu(biu)₂]²⁺ complexes are as follows: 4s, 0.50–0.54; 4p₍x,y₎, 0.49–0.53; 4p₍z₎, 0.40–0.49; 3d₍x²−y²₎, 0.54–0.66. The orbital occupation numbers calculated for the ground state of the near-planar [Cu(biu)₂]²⁻ complexes are as follows: 4s, 0.60–0.62; 4p₍x,y₎, 0.60–0.66; 4p₍z₎, 0.52–0.59; 3d₍x²−y²₎, 0.70–0.80. For the ground state of the near-planar [Cu(biu)₂] complexes, the orbital occupation numbers were calculated to be as follows: 4s, 0.54–0.60; 4p₍x,y₎, 0.54–0.63; 4p₍z₎, 0.52–0.57; 3d₍x²−y²₎, 0.62–0.74. With the several parameter sets we examined in constructing our semiempirical molecular orbital model, very little mixing between the 4s, 4p, and 3d metal orbitals was found among the occupied and low-lying virtual orbitals (molecular). The orbital occupation numbers listed above suggest significant participation of the metal 4s and 4p atomic orbitals in metal–ligand bonding in the ground states of the copper(II)–biuret complexes. However, our calculations give little evidence for significant sp²d hybridization in the ground states of these systems (although this point cannot be settled by the very approximate types of calculations performed in this study).

In the near-planar structures ($15° > \theta > -15°$ or $195° > \theta > 165°$) of the various bis(biuret)–copper(II) complexes examined here, the computed dipole strengths of the d–d transitions fall in the order d₍x²−y²₎ ← (d₍xz₎, d₍yz₎) > d₍z²₎ > d₍xy₎. However, the d₍x²−y²₎ ← d₍xy₎ transition possesses the largest magnetic dipole transition moment and exhibits, therefore, the largest dissymmetry factor ($G = 4R/D$) among the d–d transitions in each system. It is not apparent from our calculations that any single d–d transition should dominate the CD spectrum in the ligand field region (due to a consistently large rotatory strength), although the d₍x²−y²₎ ← d₍xy₎ transition is predicted to give consistently a large dissymmetry (or anisotropy) factor. In many previous studies of the chiroptical properties of pseudotetragonal transition metal complexes, it has been assumed that the d₍x²−y²₎ ← d₍xy₎ transition will yield the largest rotatory strength and will exhibit the most intense CD band in the ligand field (d–d) spectral region. Spectra–structure correlations are often based on the assignment of the most intense CD band to the d₍x²−y²₎ ← d₍xy₎ transition. Arguments based on the independent-systems and/or perturbation model[2b,c] and the results obtained in the present study suggest that this practice may not be valid. A large magnetic dipole transition moment does not guarantee that a transition will have a large rotatory strength unless a mechanism exists whereby the transition can also acquire a significant electric dipole component which is collinear with its magnetic dipole.

The rotatory strengths listed in Tables I–V are *pure electronic* rotatory strengths. Prediction of CD spectra based on electronic rotatory strengths must be made with some circumspection when the individual electronic transitions are relatively close in energy and subject to vibronic interactions of the Jahn–Teller (JT) or pseudo-Jahn–Teller (PJT) type.[13] Such interactions can effectively scramble and distort the electronic excited states involved in the transitions and lead to sign and intensity patterns in the CD spectra which cannot be interpreted in terms of specific electronic excitations. The *net* rotatory strength associated with the manifold of interacting electronic states remains invariant to PJT interactions, but assignment of specific features in the CD spectra to transitions of specific electronic parentage may no longer be valid.

The transition energies computed for the ligand field transitions of the near-planar ($\theta = 0°$) isomers of [Cu(biu)₂]²⁺ and [Cu(biu)₂]²⁻ are slightly greater than those observed experimentally for these species in solution and in the solid

state. However, the lower transition energies computed for the [Cu(biu)$_2$]$^{2+}$ complex vs. the [Cu(biu)]$^{2-}$ complex are in agreement with experiment. The d–d dipole strengths and rotatory strengths both increase as θ is varied from 0 to 90°, and the transition energies are red-shifted.

The net d–d rotatory strengths in the near-planar structures of [Cu(biu)(H$_2$O)$_2$]$^+$ and [Cu(biu)$_2$(OH)$_2$]$^-$ are identical in sign with those of the near-planar [Cu(biu)$_2$] isomers. However, the sign patterns of the d–d rotatory strengths in [Cu(biu)(H$_2$O)$_2$]$^+$ and [Cu(biu)$_2$(OH)$_2$]$^-$ are opposite (although R_{net}(d–d) is identical in sign for these two complexes).

Among the three lowest energy CT transitions in the near-planar isomers of [Cu(biu)$_2$]$^{2+}$, [Cu(biu)$_2$]$^{2-}$, and [Cu(biu)$_2$], one is computed to have only a very weak dipole strength.

B. Copper(II)–Glycine and –Glycinamide Complexes. Although the sign patterns of the d–d and CT rotatory strengths in the nearly planar structures of the copper(II)–glycine and copper(II)–glycinamide complexes are different, R_{net}(d–d) and R_{net}(CT) for these two complexes are identical in sign (Tables VI–IX). The sole source of optical activity in the cis ($\theta = 180°$) and trans ($\theta = 0°$) isomers of these complexes is conformational chirality within the chelate rings.

The amide nitrogen donors in the glycinamide ligands form strong out-of-plane π bonds with the Cu^{2+} ion, whereas in the glycine complexes the principal metal–ligand π interactions are of the Cu–O in-plane type. As was the case in the biuret complexes, we find very little mixing of the metal 4s, 4p, and 3d orbitals in the molecular orbitals computed for the [Cu(gly)$_2$] and [Cu(glya)$_2$] complexes. However, the 4s and 4p occupation numbers computed for the ground states of the various isomers lie in the range 0.35–0.60.

The signs and magnitudes of the d–d and CT rotatory strengths are very sensitive to variations in θ. The magnitudes of R_{net}(d–d) and R_{net}(CT) increase in going from $\theta = 0$ or 180° to $\theta = 90$ or 270°. Small deviations of θ from 0° (trans) or 180° (cis) generally lead to large changes in the computed rotatory strengths, and the configurational dissymmetry (or inherent dissymmetry of the extended chromophore which includes the entire carboxylate or amide moieties) generated by these deviations of θ from 0 or 180° becomes the dominant source of chirality in the complex. The chelate rings in the $\theta = +15°$ and $\theta = -15°$ isomers of [Cu(gly)$_2$] have identical conformational chiralities. However, if we ignore the chelate conformational isomerism, these two structures are enantiomeric with respect to configurational isomerism. From Table VI we note that although the sign patterns of the d–d rotatory strengths for these two structures differ significantly, the net d–d rotatory strengths very nearly bear an enantiomeric relationship one to the other. The rotatory strengths are dominated by the configurational isomerism rather than by the conformational isomerism of the chelate rings.

As was the case in the copper(II)–biuret complexes, the d$_{x^2-y^2}$ ← d$_{xy}$ transition in the near-planar [Cu(gly)$_2$], [Cu(gly)$_2$(H$_2$O)$_2$], and [Cu(glya)$_2$] complexes exhibits the weakest dipole strength (but the largest dissymmetry factor) among the d–d transitions. Additionally, in each of these complexes one of the lowest three CT transitions is computed to be nearly electric dipole forbidden.

C. Copper(II)–Alanine Complexes. The energy levels and metal–ligand bonding characteristics of the copper(II)–alanine complexes closely resemble those computed for the copper-(II)–glycine complexes. However, as a comparison of the data in Tables VI and VIII–XI reveals, the α-methyl substituent in the alanine systems exerts an enormous influence on the electronic rotatory strengths of both the d–d and low-lying CT transitions. The substituent effect completely dominates the conformational effect in these systems. The chelate ring

conformation in the [Cu(S-ala)$_2$] (CH$_3$ axial) system is identical with that in the [Cu(gly)$_2$] complexes examined here. The chelate ring conformation in the [Cu(S-ala)$_2$] (CH$_3$ equatorial) system is enantiomeric to that found in [Cu(S-ala)$_2$] (CH$_3$ axial). The net rotatory strengths calculated for these two systems are, however, identical in sign and nearly equal in magnitude (for both the cis and trans isomers). The same relationship was also found for the net CT rotatory strengths. Unlike the [Cu(gly)$_2$] cases, the cis and trans isomers of [Cu(S-ala)$_2$] are computed to have oppositely signed values of R_{net}(d–d) and of R_{net}(CT).

Our calculated results for the [Cu(S-ala)$_2$] systems suggest that the signs of the d–d CD bands of an α-alkyl-substituted amino acid complex can be correlated to the configurational dissymmetry of the asymmetric α carbon and not to the conformational dissymmetry of the chelate rings for a particular cis (or trans) form of the system. Hawkins has proposed a similar correlation based on both empirical and semiempirical considerations.[14] If the absolute configuration of the amino acid is known, the signs of the CD bands are predicted to be indicative of cis or trans isomerism within the CuO$_2$N$_2$ cluster.

D. Copper(II)–Alaninamide Complexes. The energy levels and metal–ligand bonding characteristics of the copper(II)–alaninamide complexes closely match those calculated for the copper(II)–glycinamide complexes. However, just as the α-methyl substituents (vs. chelate ring conformation) dominate the computed rotatory strengths of the d–d and CT transitions in the [Cu(S-ala)$_2$] systems, so do the α-methyl substituents dominate the computed chiroptical properties of the [Cu(S-alaa)$_2$] systems. The signs of R_{net}(d–d) and of R_{net}(CT) are identical in trans-[Cu(S-alaa)$_2$] (CH$_3$ axial) and trans-[Cu(S-alaa)$_2$] (CH$_3$ equatorial) even though the chelate ring conformations in these two isomers are enantiomeric.

The d–d transition energies in the copper(II)–alaninamide complexes are computed to be higher than those in the copper(II)–alanine complexes. This reflects the stronger interactions of the deprotonated amide nitrogen donor atoms with the Cu^{2+} ion in the alaninamide complexes compared with the Cu–O interactions in the alanine complexes. The computed transition energies are about 15–30% too high (compared to experimental data) for the d–d transitions in both the alanine and alaninamide systems. We note that whereas R_{net}(d–d) and R_{net}(CT) are predicted to have opposite signs in the trans-[Cu(S-alaa)$_2$] isomers, they are predicted to have identical signs in the trans-[Cu(S-ala)$_2$] isomers. This is in agreement with experimental observation.[15–17]

VI. Summary

The main objective of this study was to examine the sensitivity of chiroptical properties (electronic rotatory strengths and dissymmetry factors) to various structural features in the ligand environment of chiral Cu^{2+} complexes. The theoretical model adopted in carrying out this study provides only a very approximate representation of the electronic structure of the systems examined and, for this reason, the results must be considered qualitative and indicative rather than quantitative and conclusive. Of special interest were systems in which the metal ion–donor group clusters are significantly distorted away from a highly symmetrical (and achiral) geometry and in which metal–ligand π interactions are important. For such systems it is doubtful that an independent-systems and/or perturbation model is adequate for describing the chiroptical properties and it is likely that a molecular orbital model in which the systems are treated as extended chromophores will provide a more useful representation.

In addition to limitations imposed by the approximate nature of our theoretical model, the neglect of both solvent perturbations and vibronic interactions further limits the quantitative

applicability of the results obtained here. However, the qualitative usefulness of the results should not be affected by the neglect of vibronic and solvent interactions and these latter factors can be treated separately.

The results obtained for the various biuret complexes demonstrate the sensitivity of both the signs and magnitudes of the chiroptical properties to donor atom sets, configurational distortions of the chelate ring systems, and chelate ring conformation. A strong correlation between the structure variable θ and the sign and magnitude of $R_{net}(d-d)$ and $R_{net}(CT)$ was found for each of the bis(biuret) complexes. $R_{net}(d-d)$ and $R_{net}(CT)$ increase in magnitude as θ is varied from 0° (square planar CuL_4 cluster) to 90° (distorted tetrahedral CuL_4 cluster). This same variation in θ leads to significant red-shifts in the d–d transition energies and an increase in the d–d dipole strengths. A useful and reliable correlation between structure parameters and the rotatory strengths of individual transitions is not readily apparent in our calculated results. As the complexes are distorted away from near-planar geometries, assignments of individual transitions become increasingly difficult, and the sign patterns of rotatory strengths within the d–d and low-energy CT manifolds do not change continuously.

Sensitivity to the detailed nature of the metal–ligand π interactions is reflected in the opposition of signs for $R_{net}(d-d)$ and for $R_{net}(CT)$ in $[Cu(biu)_2]^{2+}$ and $[Cu(biu)_2]^{2-}$ complexes of like chirality. That is, $[Cu(biu)_2]^{2+}$ and $[Cu(biu)_2]^{2-}$ isomers of identical configurational dissymmetry exhibit $R_{net}(d-d)$ and $R_{net}(CT)$ values of opposite signs. In $[Cu(biu)_2]^{2+}$, the donor atom set is comprised of four carbonyl oxygen atoms, whereas in $[Cu(biu)_2]^{2-}$ the donor atom set is comprised of four deprotonated amide nitrogen atoms.

The results obtained for the glycine and glycinamide complexes also reflect the strong dependence of rotatory strength (sign and magnitude) upon distortions of the CuO_2N_2 (or CuN_4) cluster from a square-planar geometry. Comparison of the rotatory strengths calculated for the glycine (glycinamide) vs. alanine (alaninamide) complexes reveals that "vicinal" contributions to the d–d and CT optical activity from the α-methyl substituents in the alanine complexes completely dominate the much lesser contributions due to conformational dissymmetry in the chelate rings.

The cis and trans isomers of $[Cu(S\text{-ala})_2]$ are predicted to have $R_{net}(d-d)$ values of opposite signs. The cis and trans isomers of $[Cu(S\text{-alaa})_2]$ are also predicted to have $R_{net}(d-d)$ values of opposite signs. The computed values of $R_{net}(d-d)$ and $R_{net}(CT)$ have identical signs in the $[Cu(S\text{-ala})_2]$ complexes (cis and trans) but have opposite signs in the $[Cu(S\text{-alaa})_2]$ complexes.

References and Notes

(1) See, for example: (a) R. B. Martin in "Metal Ions in Biological Systems", Vol. 1, H. Sigel, Ed., Marcel Dekker, New York, N.Y., 1974, Chapter 4, and references therein; (b) C. J. Hawkins, "Absolute Configuration of Metal Complexes", Wiley-Interscience, New York, N.Y., 1971, Chapter 5; (c) S. F. Mason in "Fundamental Aspects and Recent Developments in Optical Rotatory Dispersion and Circular Dichroism", F. Ciardelli and P. Salvadori, Ed., Heyden and Son, New York, N.Y., 1973, Chapter 3.6.

(2) See, for example: (a) S. F. Mason, *J. Chem. Soc. A*, 667 (1971); (b) F. S. Richardson, *J. Chem. Phys.*, **54**, 2453 (1971); (c) *Inorg. Chem.*, **10**, 2121 (1971).

(3) (a) A. D. Liehr, *J. Phys. Chem.*, **68**, 665 (1964); (b) *ibid.*, **68**, 3629 (1964).

(4) A. Karipides and T. S. Piper, *J. Chem. Phys.*, **40**, 674 (1964).

(5) R. W. Strickland and F. S. Richardson, *Inorg. Chem.*, **12**, 1025 (1973).

(6) C. E. Schäffer, *Proc. R. Soc. London, Ser. A*, **297**, 96 (1968).

(7) C. E. Schäffer, *Struct. Bonding (Berlin)*, **5**, 68 (1968).

(8) R. S. Evans, A. F. Schreiner, and P. J. Hauser, *Inorg. Chem.*, **13**, 2185 (1974).

(9) H. Freeman, *Adv. Protein Chem.*, **22**, 258 (1967).

(10) E. Clementi and D. L. Raimondi, *J. Chem. Phys.*, **38**, 3686 (1963).

(11) (a) J. W. Richardson, W. C. Nieuwpoort, R. R. Powell, and W. F. Edgell, *J. Chem. Phys.*, **36**, 1057 (1962); (b) J. W. Richardson, R. R. Powell, and W. C. Nieuwpoort, *ibid.*, **38**, 796 (1963).

(12) (a) J. Webb, R. Strickland, and F. S. Richardson, *Tetrahedron*, **29**, 2499 (1973); (b) *J. Am. Chem. Soc.*, **95**, 4775 (1973); (c) F. S. Richardson and W. Pitts, *Biopolymers*, **13**, 703 (1974); (d) F. S. Richardson and D. Caliga, *Theor. Chim. Acta*, **36**, 49 (1974).

(13) (a) D. Caliga and F. S. Richardson, *Mol. Phys.*, **28**, 1145 (1974); (b) F. S. Richardson, D. Caliga, G. Hilmes, and J. J. Jenkins, *ibid.*, **30**, 257 (1975); (c) F. S. Richardson, G. Hilmes, and J. J. Jenkins, *Theor. Chim. Acta*, **39**, 75 (1975).

(14) (a) C. J. Hawkins and C. L. Wong, *Aust. J. Chem.*, **23**, 2237 (1970); (b) J. R. Goolgly, C. J. Hawkins, and C. L. Wong, *Inorg. Nucl. Chem. Lett.*, **6**, 215 (1970).

(15) (a) J. M. Tsangaris, J. W. Chang, and R. B. Martin, *J. Am. Chem. Soc.*, **91**, 726 (1969); (b) J. M. Tsangaris and R. B. Martin, *ibid.*, **92**, 4255 (1970).

(16) T. Komorita, J. Hidaka, and Y. Shimura, *Bull. Chem. Soc. Jpn.*, **42**, 168 (1969).

(17) C. Ibarra, R. Soto, L. Adan, A. Decinti, and S. Bunel, *Inorg. Chim. Acta*, **6**, 601 (1972).